Chemical Physics Letters 458 (2008) 147–151

Contents lists available at ScienceDirect

Chemical Physics Letters

journal homepage: www.elsevier.com/locate/cplett

Metal-enhanced excimer (*P*-type) fluorescence

Yongxia Zhang, Kadir Aslan, Michael J.R. Previte, Chris D. Geddes *

Institute of Fluorescence, Laboratory for Advanced Medical Plasmonics, and Laboratory for Advanced Fluorescence Spectroscopy, Medical Biotechnology Center, University of Maryland Biotechnology Institute, 725 West Lombard Street, Baltimore, MD 21201, USA

ARTICLE INFO

Article history:
Received 8 March 2008
In final form 17 April 2008
Available online 23 April 2008

ABSTRACT

In this Letter, we report the first observation of metal-enhanced excimer (*P*-type) fluorescence from pyrene. Pyrene in close proximity to silver island films (SIFs) shows enhanced pyrene excimer emission with a ≈2.5-fold higher emission intensity observed from SIFs and 5×10^{-3} M pyrene, as compared to a quartz control sample containing no silver nanoparticles. Our findings suggest two complementary methods for the enhancement: (i) surface plasmons can radiate coupled monomer and excimer fluorescence efficiently, and (ii) enhanced absorption (enhanced electric field) further facilitates enhanced emission. This observation is helpful in our laboratory's continued goal to develop a unified plasmon–luminophore description.

1. Introduction

Fluorescence is widely used in biology, microscopy imaging, medical research and diagnosis [1–3]. Improving fluorescence detectability remains a great challenge, in part due to the quantum yield and photostability of the fluorophore, and the autofluorescence of the sample. In this regard, there has been significant recent interest in using sub-wavelength sized metallic nanostructures to favorably modify the spectral properties of fluorophores and to amplify the fluorescence emission [4], modify fluorescence lifetimes [5], and protect against photobleaching [6]. Currently, there are several explanations for the near-field interactions of fluorophores with metallic nanoparticles. The photophysical properties of the fluorophores are thought to be modified by a resonance interaction in close proximity to surface plasmons, which also gives rise to a modification of the fluorophore's radiative decay rate [7]. This description was fueled by earlier workers who had shown increases in fluorescence emission coupled with a simultaneous drop in radiative lifetime [5]. However, our laboratory's current interpretation of the metal–fluorophore interactions (phenomenon named metal enhanced fluorescence, MEF by Geddes) is described by a model whereby non-radiative energy transfer occurs from excited distal fluorophores, to the surface plasmon electrons in non-continuous films. In essence a fluorophore induced mirror dipole in the metal [8,9]. The surface plasmons in turn, radiate the emission of the coupling fluorophores (Fig. 1 top). This explanation has been facilitated by the observation of surface plasmon coupled fluorescence (SPCF), whereby fluorophores distal to a continuous metallic film can directionally radiate fluorophore emission at a unique angle from the back of the film [10].

Nearly all of our previous studies in MEF were exclusively focused on intramolecular monomer fluorescence emission [9]. In this work, we show that surface plasmons can radiate and amplify intermolecular excimer fluorescence. The term 'excimer' is an abbreviation for an excited state dimer which is formed between the ground state (M) and lowest electronically excited singlet state (M^*) of a species. The aromatic molecule pyrene is well-known for forming an excimer. After Förster and Kasper first identified an excimer of pyrene in solution in 1953, pyrene has subsequently attracted a lot interest from photophysicists. The rates and pathways associated with the excimer system are shown in Scheme 1 [11]. The excimer E^* is a relatively stable complex between one excited molecule of pyrene and another in its ground state, with a binding energy of 38–42 kJ mol^{-1} in non-viscous solvents. The formation process, K_1 and K_2 are related to the diffusion-controlled rate of the donor/acceptor system [11]. The fluorescence spectra of highly concentrated solutions of pyrene show two distinct emission bands. The fine structured band below 400 nm corresponds to emission from the singlet excited state monomer, M^*. The broad band centered ≈ 470 nm is characteristic of the emission from 'excited dimers' or excimers. The monomer and excimer lifetimes of pyrene in alcohols were measured previously by Scaiano and Focsaneanu [12] as ≈100 ns and 50 ns, respectively.

Pyrene fluorescence has been of great interest and a useful tool to biologists and biochemists alike. For example, pyrene has been used to probe RNA folding and DNA duplex formation by monitoring the monomers and excimer emission fluctuations that arise from local base stacking and the quenching effect [13]. Pyrene

Abbreviations: MEF, metal enhanced fluorescence; $MEPT_E$, metal enhanced *P*-type excimer Emission; $MEPT_m$, metal enhanced *P*-type monomer emission.

* Corresponding author. Fax: +1 4107064600.
E-mail address: geddes@umbi.umd.edu (C.D. Geddes).

0009-2614/$ - see front matter © 2008 Elsevier B.V. All rights reserved.
doi:10.1016/j.cplett.2008.04.083

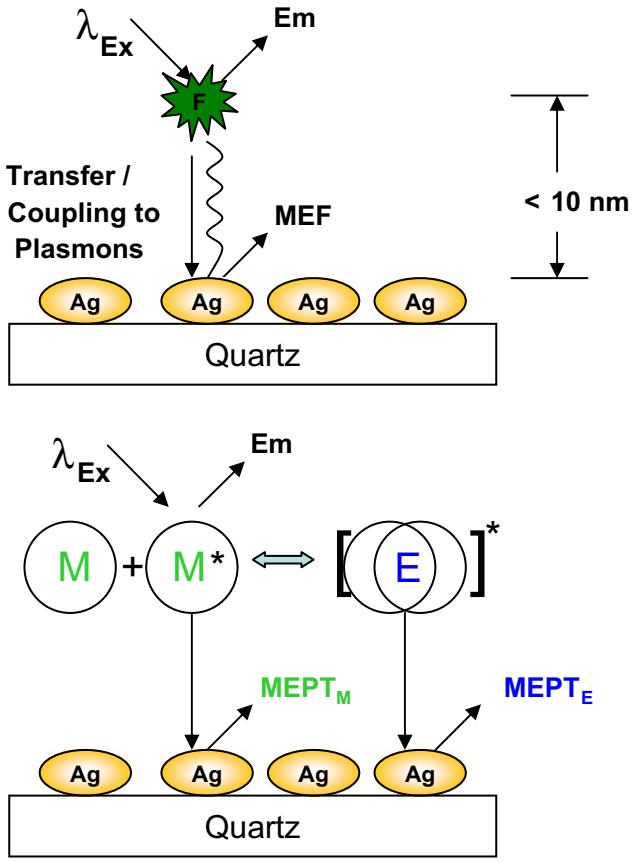

Fig. 1. Graphical representation of current interpretation for metal-enhanced fluorescence on silvered quartz (top) and metal-enhanced *P*-type fluorescence (bottom). F – fluorophore, MEF – metal-enhanced fluorescence, Ag – silver nanoparticles, $MEPT_m$ – metal enhanced *P*-type monomer emission, $MEPT_E$ – metal enhanced *P*-type excimer emission. M – pyrene monomer, E – pyrene excimer.

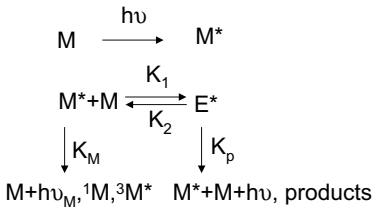

Scheme 1. Rates and pathways associated with the pyrene excimer system. M^* represents excited singlet pyrene molecules, M ground state molecules, and E^* an excited state complex. K_1 and K_2 diffusion-controlled rate of the donor/acceptor system.

has also been used for the selective detection of cellular mRNA by yielding a strong excimer emission at 485 nm in the presence of the target [14]. Pyrene has been widely used in membrane biophysics, where the pyrene (lipid-linked) is used as a probe to provide information on membrane fluidity and behavior of single lipid molecular conformation and movement [15]. However, the sensitivity of these approaches of the singly labeled pyrene probe is typically more dependent on the excimer emission, due to the inherently high biological autofluorescence in the pyrene monomer emission region.

In this Letter, we subsequently report our observations of MEF from pyrene when placed in close proximity to SIFs. The excimer fluorescence emission was ≈2.5-fold brighter from SIFs as compared to a quartz control substrate. A reduction in the lifetime of the excimer was also observed in close proximity to SIFs (19.1 ns on quartz and 3.64 ns on SIFs), which suggests that the excimer emission enhancement is in part due to coupling-to and emission-from surface plasmons (Fig. 1 bottom).

2. Experimental

2.1. Materials

Silver nitrate (99.9%), sodium hydroxide (99.996%), ammonium hydroxide (30%), D-glucose, ethanol (HPLC/spectrophotometric grade), pyrene, cyclohexane were obtained from Sigma–Aldrich. Quartz (75 × 25 mm) slides were bought from Ted Pella Inc. All chemicals were used as received.

2.2. Methods

SIFs (size is ≈100 nm, AFM image not shown) were prepared according to the previously published procedure [16]. Three hundred microlitre of pyrene dissolved in cyclohexane was sandwiched between both the quartz slides and the SIFs coated quartz slides, respectively. Fig. 2 top shows the experimental sample geometry. The monomer and excimer fluorescence spectra were collected on a Varian Cary Eclipse fluorometer at an angle of 45° to the surface. Excitation light was incident to the bottom of the slides surface with excitation of 330 nm, slit width ≈20 nm.

2.2.1. FDTD simulations

FDTD simulations were used to determine the electric field intensities at the surface of a 100 nm silver nanoparticle and is described in detail elsewhere [17].

2.2.2. Luminescence lifetime analysis

Fluorescence lifetimes were measured using the time-correlated single photon counting technique (TCSPC), a PicoQuant modular fluorescence lifetime spectrometer (Fluo Time 100) with a

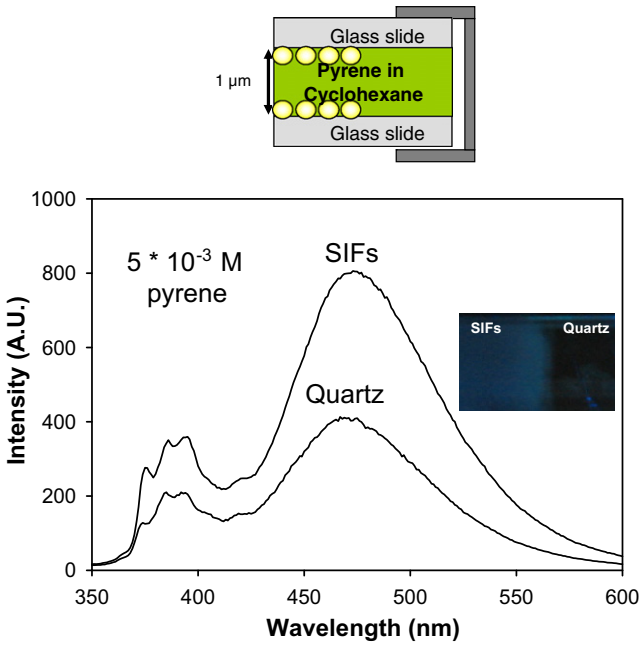

Fig. 2. Sandwich experimental setup (top). *P*-type fluorescence emission spectra, λ_{ex} = 330 nm, for pyrene sandwiched between two silvered and unsilvered quartz slides at room temperature, (bottom), and real-color photographs of excimer emission taken through a 450 nm longpass filter (bottom photograph insert).

PicoQuant 280 nm light source. The intensity decays were analyzed in terms of the multi-exponential model:

$$I(t) = \sum_i \alpha_i \ \exp(-t/\tau_i) \quad (1)$$

where α_i are the amplitudes and τ_i are the decay times, $\sum_i \alpha_i = 1.0$. The fractional contribution of each component to the steady state intensity is given by

$$f_i = \frac{\alpha_i \tau_i}{\sum_j \alpha_j \tau_j} \quad (2)$$

The mean lifetime of the excited state is given by

$$\bar{\tau} = \sum_i f_i \tau_i \quad (3)$$

and the amplitude-weighted lifetime is given by

$$\langle \tau \rangle = \sum_i \alpha_i \tau_i \quad (4)$$

The values of α_i and τ_i were determined by a nonlinear least squares impulse reconvolution with a goodness-of-fit χ^2 criterion.

3. Results and discussion

Due to transitions from the lowest vibrational level of the monomer excited state to several vibrational levels of the ground state, the fluorescence emission spectrum of the monomer of pyrene from quartz and SIFs has fine structured bands at 370 nm, while the broad excimer emission yields an unstructured band ≈470 nm [18]. Enhanced monomer emission (≈1.5-fold brighter) and excimer fluorescence emission (≈2.5-fold brighter) was typically observed from the SIFs as compared to a quartz control substrate (Fig. 2 bottom), containing no silver nanoparticles. These findings of metal-enhanced monomer and excimer fluorescence of pyrene are consistent with our previous reported findings for structured and unstructured S_1 emission for fluorophores sandwiched between silver nanostructures [19]. Metal-enhanced excimer fluorescence can also be seen visually (Fig. 2 insert) from real-color photographs taken through a 450 nm longpass filter.

Pyrene monomer fluorescence (Fig. 3, top) and excimer (Fig. 3, bottom) maximum emission intensity versus $\log_{10}$ pyrene concentration are enhanced in the presence of SIFs. Excimer intensities are 2.5-fold higher at concentrations $>10^{-3}$ M (Fig. 3, bottom) in the presence of the silver nanoparticles. In this regard, it should be noted that the observed enhancement is also effected by the quantum yield of the fluorophore and the type of the metal nanostructures and the distance between the fluorophores and metal nanostructures. The true metal-enhanced monomer/excimer fluorescence enhancement factors are much higher than observed. This is because a sample thickness is of ~1 μm and an enhanced interaction region <20 nm, then only ≈4% of the sample is actually within the MEF enhancement region, as depicted in Fig. 2 top. Therefore, the true enhancement factor for excimer is 25–100. It is also important to note that since it is beyond the scope of this study we did not attempt to make a comparison of enhancement factors for MEF and surface enhanced raman scattering (SERS) due the major physical differences in both phenomena.

In Fig. 4, the metal enhancement factors for monomer and excimer versus $\log_{10}$ pyrene concentration are shown and are generally greater than 1, implying that there is a net plasmon enhancement in the system (Fig. 1 bottom) where both monomer and excimer are both plasmon enhanced. Interestingly, a plot of the excimer enhancement factor divided by the monomer enhancement factor (Fig. 4 insert) reveals that the excimer bands are enhanced more than the monomer bands. This result can be explained according to the current interpretation of MEF [16], whereby the excimer can couple more effectively to the scattering portion of the metal particle extinction at this wavelength. In essence, fluorophores whose emission spectra overlap with the scattering spectra of the metal, show larger enhancement factors.

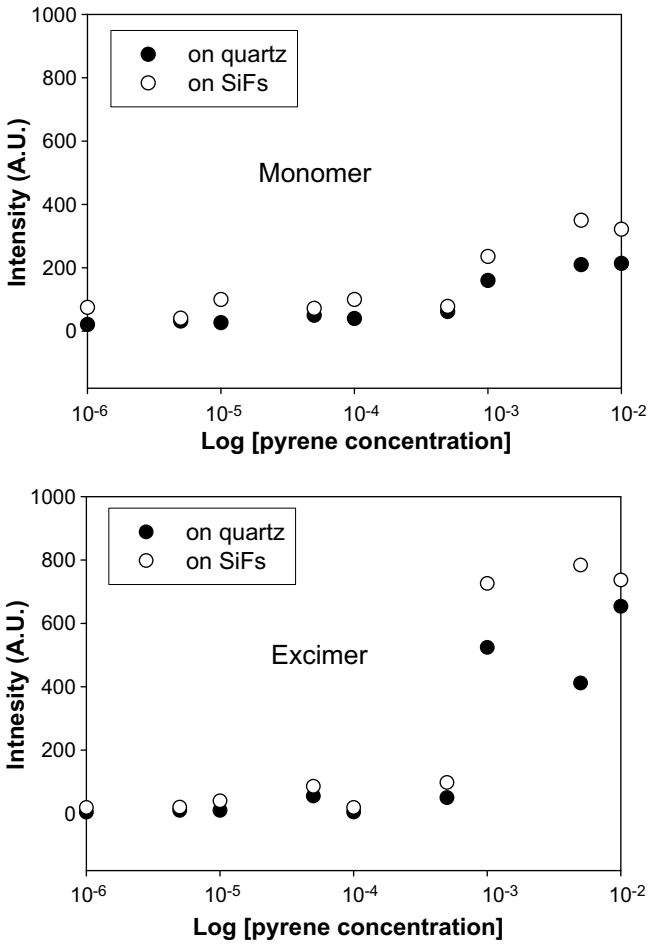

Fig. 3. *P*-type monomer fluorescence maximum emission intensity versus Log 10 pyrene concentration (top) and excimer maximum fluorescence emission intensity versus Log 10 pyrene concentration (bottom).

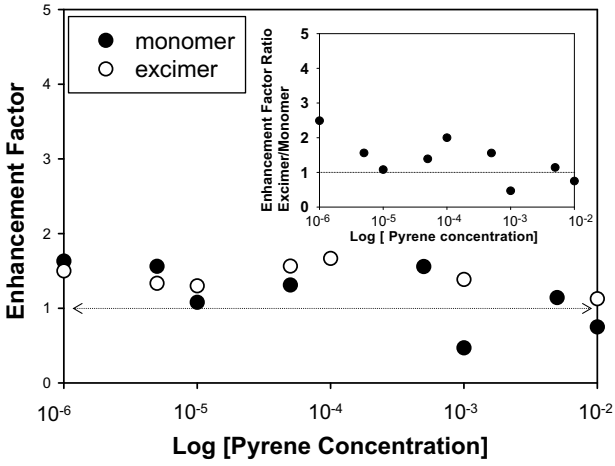

Fig. 4. Metal enhancement factor for monomer and excimer versus Log_{10} pyrene concentration. Enhancement factor excimer/monomer versus Log_{10} pyrene concentration (insert).

At present we suggest two complementary effects for the enhancement: (i) surface plasmons can radiate coupled-excimer fluorescence efficiently, and (ii) enhanced absorption facilitates enhanced emission. In this regard, we studied the absorption of pyrene in the presence and absence of SIFs (Fig. 5 top). SIFs and glass without pyrene were used as reference backgrounds for the pyrene absorption measurements, respectively. It can be seen that pyrene has a larger absorbance on SIFs as compared to that on quartz. When a luminophore is placed near-to metal, there is often a very strong net absorption effect caused by the localized enhanced electromagnetic field of the incident excitation field. Conductive metallic particles can modify the free space absorption condition in ways that increase the photonic mode density and incident electric field felt by a luminophore. Since enhanced electromagnetic

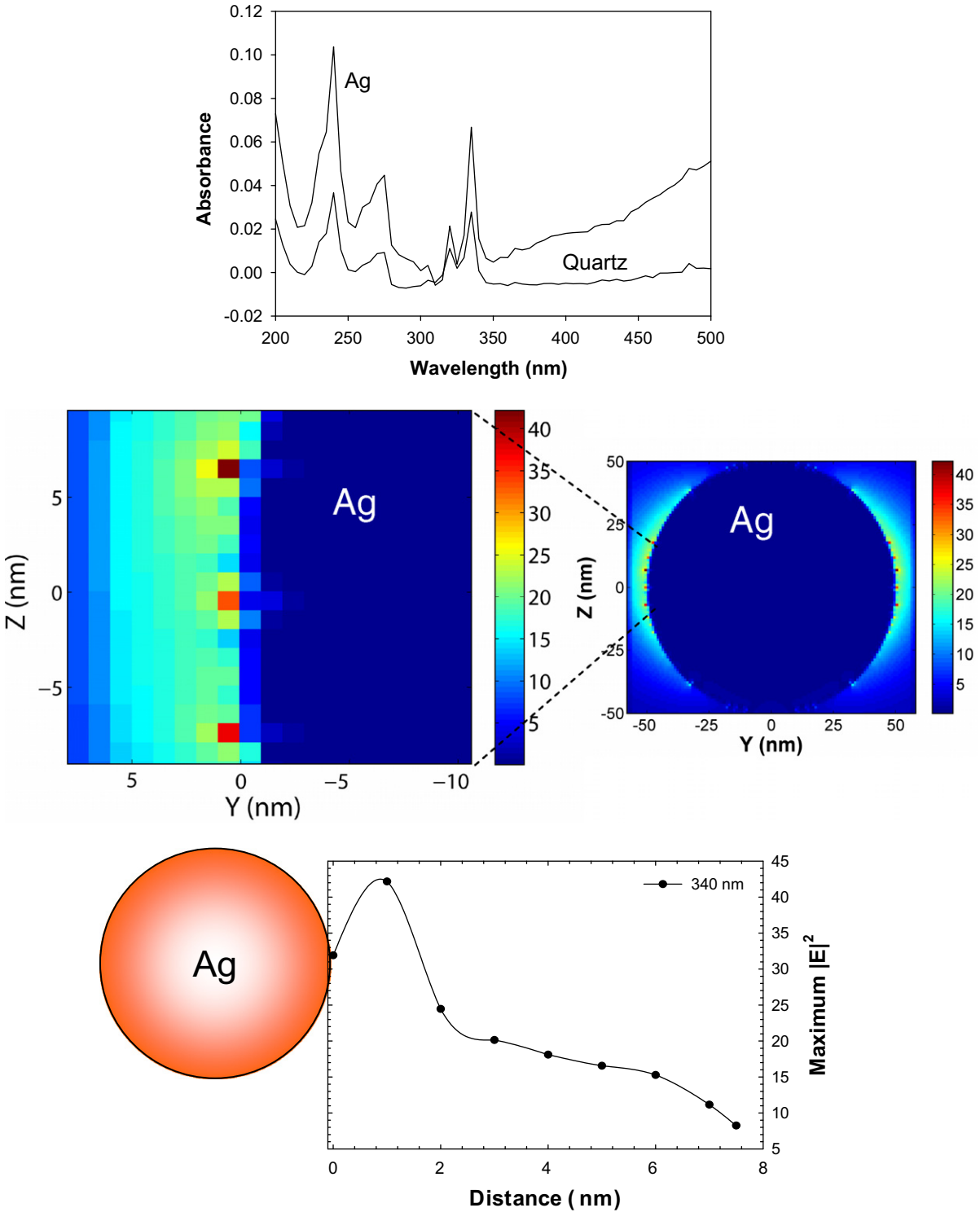

Fig. 5. Absorption spectra of pyrene (10^{-3} M in cyclohexane) immobilized in a sandwich between two silvered and unsilvered slides respectively (top). Magnified region of the E^2 field intensity distribution in the *YZ* plane at the surface of a 100 nm silver nanoparticle (middle left) and the field distribution around the extent of the nanoparticle (middle right). Maximum E-field distribution versus distance from the surface of the sphere $y = 0$ to $y = 8$ nm (bottom).

Table 1
Fluorescence intensity decay analysis (10–4 M pyrene)

	τ_1 (ns)	α_1 %	τ_2 (ns)	α_2 %	$\langle\tau\rangle$ (ns)	τ (ns)	χ^2
Pyrene on quartz	31.6	0.59	0.49	0.41	19.1	31.28	1.151
Pyrene on SIFs	19.1	0.16	0.74	0.84	3.64	15.96	1.224

τ – *mean lifetime,* $\langle\tau\rangle$ – *amplitude-weighted lifetime. SIFs – silver island films.* $\alpha_1 + \alpha_2 = 100$; α_n – amplitudes. Ex: 280 nm. Emission was recorded through a 295 nm longpass filter.

fields in proximity to metal nanoparticles are the basis for the increased system absorption in MEF [16], we have used finite difference time domain (FDTD) methods to simulate the E-field distributions around silver nanoparticles, and as a function of distance to the surface of a silver sphere (100 nm) $y = 0$ to 8 nm (Fig. 5 middle and bottom). As we can see, the electric field around the silver nanoparticles is quite intense and decays as we move further way from the silver nanoparticle. Hence, pyrene monomers and excimers within 10 nm of the SIFs are likely to show enhanced absorption properties, as experimentally verified in the absorption spectra (Fig. 5 top). It should be noted that an enhanced E-field only influences the excitation rate of a fluorophore by an effective change in its absorption cross-section in the metal–fluorophore coupled system, but does not influence its emissive lifetime.

In addition, we have also measured the fluorescence lifetime which is only affected by the emission rate in close proximity to SIFs. The respective lifetimes were calculated from the decay data (data not shown), using a bi-exponential decay curve analysis. We observed a reduced fluorescence amplitude-weighted lifetime ($\langle\tau\rangle_{\text{on SIFs}} = 3.64$ ns) for fluorophores near-to silver as compared to the quartz control sample ($\langle\tau\rangle_{\text{on quartz}} = 19.1$ ns) (Table 1). These findings are consistent with our previously reported findings and trends for fluorophores sandwiched between silver nanostructures, and suggest that in addition to an enhanced absorption, pyrene emission is also plasmon coupled and radiated by the nanoparticles themselves [16] as depicted in Fig. 1 bottom.

4. Conclusions

In this Letter, we report the first observation of metal-enhanced excimer fluorescence, which is thought due to both enhanced absorption and surface plasmons radiating excimer fluorescence efficiently. Pyrene in close proximity to SIFs can undergo enhanced monomer and excimer fluorescence, as compared to an identical control sample containing no silver. This observation is helpful in the future development of high quantum yield and photostable probes for biophysical applications, as well as for our laboratory's continued efforts to develop a unified plasmon–luminophore description.

Acknowledgements

The authors would like to thank the IoF, MBC, UMBI and the NIH-NINDS R21 NS055187 for support.

References

[1] H. Andersson, T. Baechi, M. Hoechl, C. Richter, J. Microsc.–Oxford 191 (1998) 1.
[2] R.R. Alfano, A. Pradhan, G.C. Tang, S.J. Wahl, J. Opt. Soc. Am. B–Opt. Phys. 6 (1989) 1015.
[3] A.C. Croce, A. Ferrigno, M. Vairetti, R. Bertone, I. Freitas, G. Bottiroli, Photochem. Photobiol. Sci. 3 (2004) 920.
[4] A.M. Glass, P.F. Liao, J.G. Bergman, D.H. Olson, Opt. Lett. 5 (1980) 368.
[5] D.A. Weitz, S. Garoff, C.D. Hanson, T.J. Gramila, J.I. Gersten, Opt. Lett. 7 (1982) 89.
[6] S. Garoff, D.A. Weitz, M.S. Alvarez, J.I. Gersten, J. Chem. Phys. 81 (1984) 5189.
[7] J. Gersten, A. Nitzan, J. Chem. Phys. 73 (1980) 3023.
[8] P.C. Das, A. Puri, Phys. Rev. B 65 (2002).
[9] C.D. Geddes, J.R. Lakowicz, J. Fluores. 12 (2002) 121.
[10] T. Liebermann, W. Knoll, Colloid Surface A–Physicochem. Eng. Asp. 171 (2000) 115.
[11] M. Okamoto, J. Phys. Chem. A 104 (2000) 5029.
[12] K. Focsaneanu, J.C. Scaiano, Photochem. Photobiol. Sci. 4 (2005) 817.
[13] N.S. Patrick Conlon, et al., J. Am. Chem. Soc. 130 (2008) 336.
[14] A.A. Marti, X. Li, S. Jockusch, A. Li, B. Raveendra, N.J. Turro, Nucl. Acid Res. 34 (2006) 3161.
[15] P. Somerharju, Chem. Phys. Lipids 116 (2002) 57.
[16] K. Aslan, Z. Leonenko, J.R. Lakowicz, C.D. Geddes, J. Fluores. 15 (2005) 643.
[17] Y. Zhang, K. Aslan, J.R.P. Previte, D.C. Geddes, PNAS 105 (2008) 1798.
[18] P.C.J.H.W.P.C. Johnson, H.W. Offen, J. Chem. Phys. 59 (1973) 801.
[19] Y. Zhang, K. Aslan, M.J. Previte, C.D. Geddes, Appl. Phys. Lett. 90 (2007) 053107.